

ARMY RESEARCH LABORATORY



UV/Vis Emission From Shock-Loaded Liquid Propellant XM46

by M. J. McQuaid,
J. L. Watson, and D. L. Pilarski

ARL-TR-1672

May 1998

19980618 175

Approved for public release; distribution is unlimited.

DTIC QUALITY INSPECTED 1

The findings in this report are not to be construed as an official Department of the Army position unless so designated by other authorized documents.

Citation of manufacturer's or trade names does not constitute an official endorsement or approval of the use thereof.

Destroy this report when it is no longer needed. Do not return it to the originator.

Army Research Laboratory

Aberdeen Proving Ground, MD 21005-5066

ARL-TR-1672

May 1998

UV/Vis Emission From Shock-Loaded Liquid Propellant XM46

M. J. McQuaid, J. L. Watson, D. L. Pilarski
Weapons and Materials Research Directorate, ARL

Abstract

In flyer plate impact experiments conducted to study the response of the liquid propellant XM46 to shock loading, it had been observed that, in cases where the sample reacted violently, a luminous wave would travel at high velocity across a free-surface or container boundary prior to significant acceleration of material. This report presents the results of experiments in which the ultraviolet (UV) and visible (Vis) radiation from this wave were spectrally resolved. The emission spectrum was found to be a broad, nearly structureless continuum that extends from a short wavelength onset near 400 nm to the long wavelength limit of the detection system at approximately 800 nm. It is considered that this signature is attributable to emission from electronically excited NO_2 . Mechanisms that might explain the experimental observations are discussed.

Acknowledgments

The experiments described in this report were conducted with the assistance of D. Saunders, T. Sluss, J. Lundy, and D. Serrano. The spectroscopic equipment was loaned to us by Dr. A. Birk. The authors are also indebted to Drs. R. Frey and N. Klein for helpful discussions on shock physics and hydroxylammonium nitrate (HAN)-based propellant chemistry, and Dr. K. McNesby for reviewing the manuscript.

INTENTIONALLY LEFT BLANK.

Table of Contents

	<u>Page</u>
Acknowledgments	iii
List of Figures	vii
1. Introduction	1
2. Experimental Considerations	3
3. Results and Discussion	7
4. Summary	12
5. References	13
Distribution List	15
Report Documentation Page	17

INTENTIONALLY LEFT BLANK.

List of Figures

<u>Figure</u>		<u>Page</u>
1.	Experimental Setup	4
2.	High-Speed-Film Record of a Representative Experiment	6
3.	Photodiode Response for the Experiment Shown in Figure 2	7
4.	Emission Spectrum Associated With Bubble Collapse and Comparison to a Black-Body Emitter at 2,800 K	8
5.	Emission Spectrum Associated With the Luminous Wave and Comparison to a Black-Body Emitter at 3,800 K	9

INTENTIONALLY LEFT BLANK.

1. Introduction

Reduction of propellant vulnerability through storage compartment design requires knowledge of the mechanisms that can induce a violent propellant response. The Army's attempt to develop the regenerative liquid propellant gun (RLPG) concept VI-C as the gun propulsion system for the Crusader (howitzer) program prompted considerable effort to establish design guidelines for fielding the hydroxylammonium nitrate (HAN)-based liquid monopropellant XM46 [1-7]. A particular concern was the effect of a shaped charge jet penetrating an XM46-filled container [1-4]. If a jet penetrates the propellant, a bow shock is produced that propagates through the liquid to container walls and possibly a free surface. The consequent interactions produced at these interfaces have the potential to generate (localized) high temperatures and cavitation. Under certain conditions XM46, which is generally very insensitive, will react explosively when exposed to such threats.

One of the primary methods for studying fundamental processes involved in a shaped charge jet penetration is flyer plate impact experiments [5-7]. From the standpoint of understanding shock-induced initiation mechanisms, these experiments are preferred to experiments in which shaped charge jets are actually fired because they produce a nearly planar shock wave whose strength and duration can be well controlled and characterized. "Standard" flyer plate impact experiments conducted in support of the Crusader effort involved explosively launching a metal plate (with dimensions on the order of 150 mm \times 150 mm \times 10 mm thick) to velocities in the range of 0.3 to 2.0 mm/ μ s. Typical diagnostic approaches employed to study initiation mechanisms were piezoelectric pin arrays (to measure the shock wave's velocity) and high-speed photography. Shock velocity data were reduced to provide Hugoniot equation of state parameters for the propellant [5], and the results provided evidence for chemical energy release at high shock loads. High-speed photography provided a basis for identifying material failure and/or spall and the identification of reaction initiation sites. From this data, Watson and Pilarski [6] identified a five-step process leading to violent reaction: (1) shock loading, (2) the introduction of voids via release and cavitation, (3) ignition via compressive or shear heating, (4) induction (with no significant gas evolution), and (5) chemical reaction (with gas evolution and rapid acceleration of materiel).

The current study was one of several project manager (PM)-Crusader-supported efforts in which spectroscopically based techniques were employed to identify the role of chemistry in the initiation process [7]. Such studies were prompted by the fact that neither the shock velocity measurements nor the high-speed-framing camera records indicate that XM46 changes (chemically) as a direct result of shock loading to pressures less than 7 GPa. However, the propellant will react violently when shocked to as little as 1 GPa if cavitation (step 2) occurs. The relatively long delay between shock loading and rapid acceleration of materiel, coupled with the fact that XM46 combustion is inefficient at pressures less than 10 MPa, suggests that the propellant decomposes to an intermediate chemical state that sets the stage for a violent response. Knowledge of such chemistry may suggest alternate approaches to reducing propellant vulnerability and may also be relevant to addressing the issue of long-term storage of XM46 that has been subjected to a strong, but noninitiating, shock load.

Most of the spectroscopic efforts undertaken with PM-Crusader support involved attempts to identify the induction of chemical-intermediate formation during the initial pass of the shock wave (i.e., step 1 of the Watson and Pilarski mechanism). Baker and coworkers [8] (U.S. Army Research Laboratory [ARL]) developed an experiment in which an XM46 sample could be shocked without subsequent exposure to rarefaction waves, preventing cavitation. Recovered samples were probed via Fourier transform infrared (FTIR) absorption spectroscopy to identify chemical changes. Based on limited data, these researchers concluded that no significant irreversible decomposition or reaction occurs when virgin XM46 is shocked to pressures less than 2.4 GPa. McQuaid and coworkers [9] (ARL) attempted to detect chemical-intermediate formation in real time using Raman spectroscopy, and evidence for the production of NO_2 was observed. However, cavitation may have played a role in the process leading to this result. Fishburn and Lu [7] and Idar and Pederson [10] (Los Alamos and Rutgers, respectively) were unable to draw conclusions from "standard" flyer plate impact experiments in which real-time, near-IR absorption spectroscopy was employed. Thus, the direct production of chemical intermediates by shock loads less than 7 GPa has yet to be established. At the same time, it would seem premature to rule out this possibility based on the studies available.

The study reported here is more directly related to the induction phase (step 4 of the Watson and Pilarski mechanism). The induction phase is a period immediately following the appearance of a visible hot spot and lasting up to tens of microseconds, during which the propellant undergoes reactions that generate little gas, but produce a final (chemical intermediate) state capable of reacting explosively. The induction phase is marked by the propagation of a luminous (white) wave that travels at high velocity across free-surface or container boundaries. In the experiments reported here, radiation from the wave was collected with an optical fiber and spectrally resolved with a UV/Vis optical multichannel analyzer (OMA). The spectrum associated with the wave was found to be a broad, nearly structureless continuum that extends from approximately 400 nm to the long wavelength limit of the detection system at approximately 800 nm. The spectrum is consistent with emission from electronically excited NO_2 . Mechanisms that might explain the experimental observations are discussed.

2. Experimental Considerations

A schematic diagram of the experimental setup is shown in Figure 1. A 100 mm \times 100 mm \times 50 mm container was constructed with 6-mm-thick polymethylmethacrylate (PMMA) sidewalls and an aluminum base plate. It was completely filled with XM46 (60.9 wt-% HAN, 19.1 wt-% triethanolammonium nitrate (TEAN), and 20.0 wt-% water), a PMMA lid placed on top, and a bubble purposely introduced along one edge to provide an initiation site. A 6.25-mm-thick aluminum flyer plate was explosively launched to a velocity of 1.2 mm/ μs using a plane wave generator, producing an impact that generated an initial shock pressure of approximately 5 GPa in the XM46. A high-speed-framing camera (Beckman-Whitley, Model 189) was employed in initial experiments to establish the best means of conducting the spectroscopic investigation. This camera utilizes a gas-turbine-driven prism to control the exposure of a strip of 35-mm (color) film. An interframe time of 4 μs and an exposure duration of 1.3 μs were selected for recording these experiments.

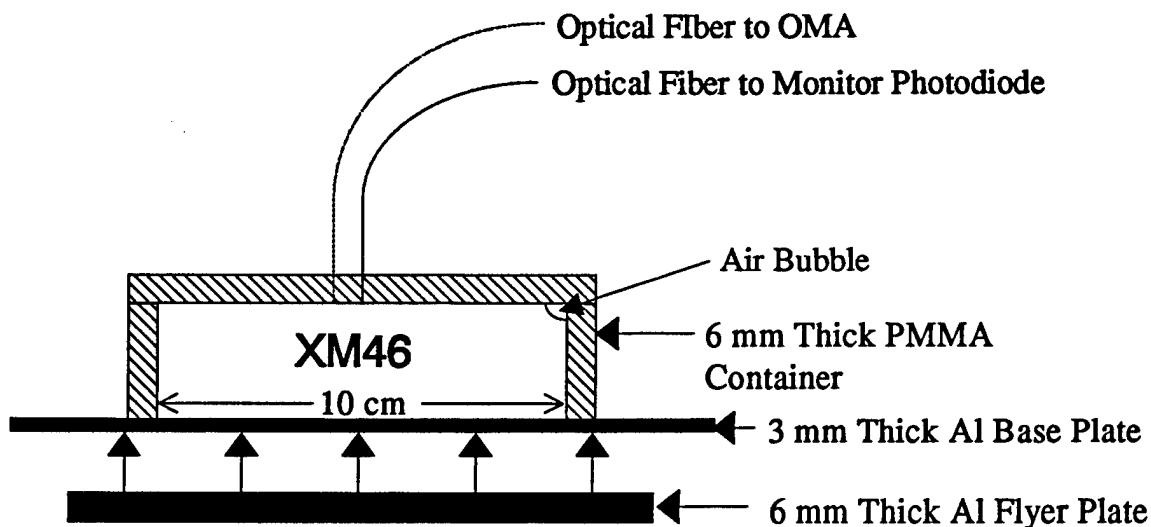


Figure 1. Experimental Setup.

Two optical fibers were mounted into the lid of the container, and their ends were positioned flush with the inner wall. The fiber positioned closest to the bubble was coupled to a photodiode to monitor total visible light levels; the photodiode response provided a trigger signal for other instrumentation. The other fiber (3M, FP-600-UHT), which was approximately 10 m long, was directed to the monochromator (ISA, HR-320) of an OMA system (Princeton Instruments, Model ST-1000 controller and Model IPDA-1024 intensified photodiode array). The 1024-element photodiode array responds to radiation in the wavelength range from 200 to 800 nm.

Since the output beam (divergence) of the fiber ($NA = 0.4$) could be reasonably collected by the monochromator optics ($f\text{-number} = 4.2$), the end of the fiber was simply positioned at the entrance (slit) of the monochromator, the slit being employed solely as a guide for alignment. The monochromator was equipped with a 150 grooves/mm grating (blazed at 500 nm), which, operated in first order, provided an approximately 500-nm spectral detection window with a resolution of about 4 nm (full width at half maximum [FWHM]). The window was typically set to monitor from 250 nm to 750 nm. Wavelength calibration for the system was established by reference to the spectral lines of a mercury-vapor lamp. The wavelength-dependent intensity response of the fiber-optic-OMA combination was determined by reference to a tungsten-ribbon lamp (Eppley) with a National Bureau of Standards (now the National Institute for Standards and Technology [NIST])

traceable radiance vs. wavelength calibration. We note that, even though the fiber optics were selected based on their having relatively good UV transmission properties (for fiber optics) and that they, in principle, allowed detection of spectral features at wavelengths as low as 200 nm, the attenuation per meter of fiber increases significantly as the wavelength decreases below 400 nm. Coupled with the fact that the spectral radiance of the calibration lamp decreases with wavelength over several orders of magnitude, a large uncertainty attends the calculation of the system response function for $\lambda < 350$ nm. Similarly, the sensitivity of the diode array falls off rapidly as the wavelength increases above 750 nm, and the calculated response function for the long wavelength extreme of the system has a high degree of uncertainty. Thus, the spectral analysis described next focused on the 350 nm to 750 nm wavelength regime.

Because the frequency at which the emission could be sampled by the OMA system was limited to less than 250 Hz, and the phenomena of interest occurred within 20 μ s, only a single spectrum could be acquired per experiment. This restricted our ability to temporally resolve the process, and the timing scheme (trigger level, delay of the high-voltage intensifier [exposure] gate following the trigger, and exposure duration) deserves comment. The primary consideration was timing the high-voltage gate of the intensifier to coincide with the arrival of the reaction wave at the fiber end. Our approach, which was to trigger the gate based on the response of the monitor photodiode, was complicated by shot-to-shot variations in the onsets and intensities of emission from the collapsing bubble and the wave. The implementation of the approach, which was to set the trigger at a photodiode response level that was between the maximum level expected from the collapsing bubble and the maximum level expected from the reaction wave (see Figures 2 and 3) became reliable only after considerable experimentation. We were, however, fortunate that two spectra were “inadvertently” acquired during bubble collapse, since we might not have collected such spectra otherwise, and they proved to be instructive.

As for setting the exposure delay and duration, the high-speed-film records suggest that the visible spectral content of the wave is independent of position and time (see Figure 2), and, thus, our main goal in setting these parameters was to obtain maximum intensity levels in the middle of the diode array’s dynamic range. For the given trigger level, this was achieved by setting the delay as

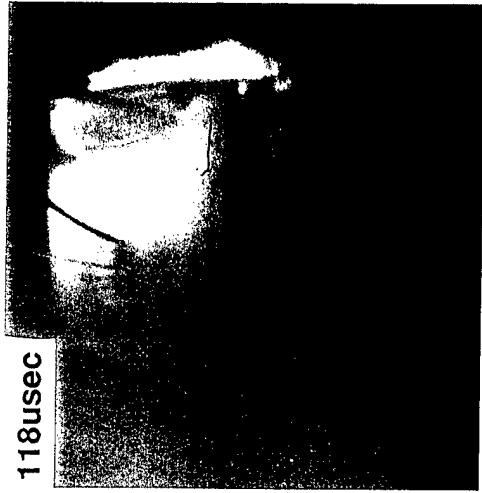


Figure 2. High-Speed-Film Record of a Representative Experiment.

short as possible (i.e., the inherent, nanosecond-scale delay of the electronics) and setting the gate width to $0.25 \mu\text{s}$. The photodiode response and the timing of the gate were recorded on a digital waveform recorder (Nicolet, Model Pro 60). Spectra were recorded directly to a personal computer.

3. Results and Discussion

A representative high-speed-film record acquired from these experiments is shown in Figure 2. Two distinct light-producing events are observed. The first, which onsets $110 \mu\text{s}$ after the trigger to launch the flyer plate, corresponds to the collapse of the bubble. The second, which corresponds to the propagation of the luminous wave across the XM46-container boundary, is observed to cross in front of the fiber optics between 118 and $122 \mu\text{s}$. As shown in Figure 3, these events are clearly identifiable in the record of the monitor photodiode response.

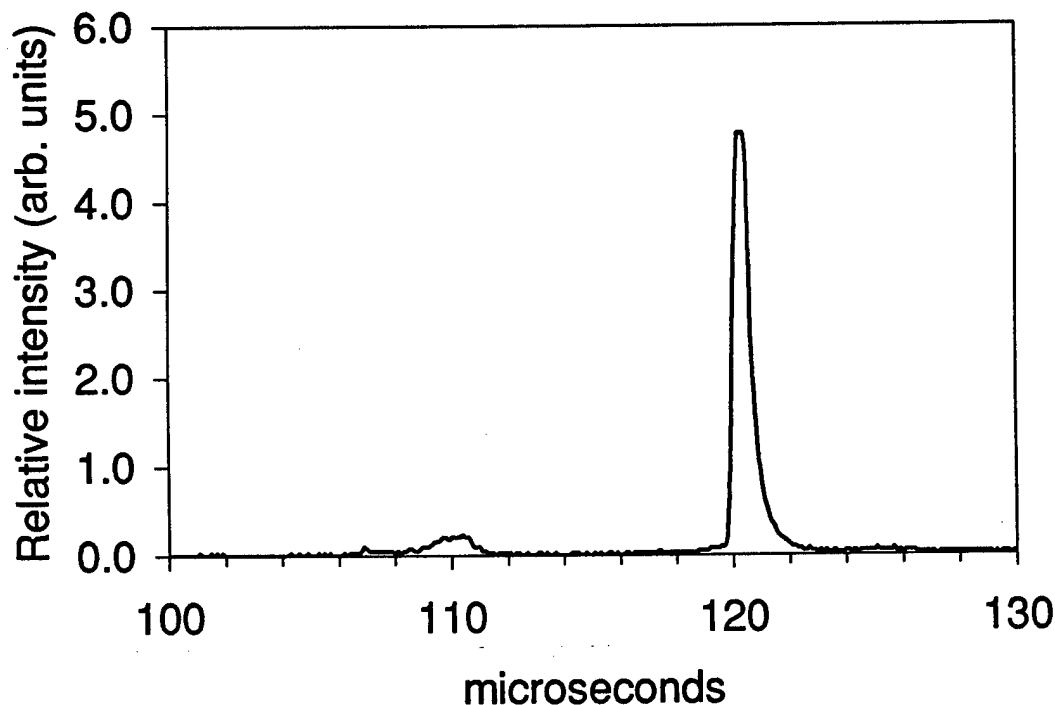


Figure 3. Photodiode Response for the Experiment Shown in Figure 2.

An average of the two spectra recorded during initial bubble collapse is shown in Figure 4. This spectrum is well fit by a black-body radiation model with arbitrary irradiance (y-scale) units. (We

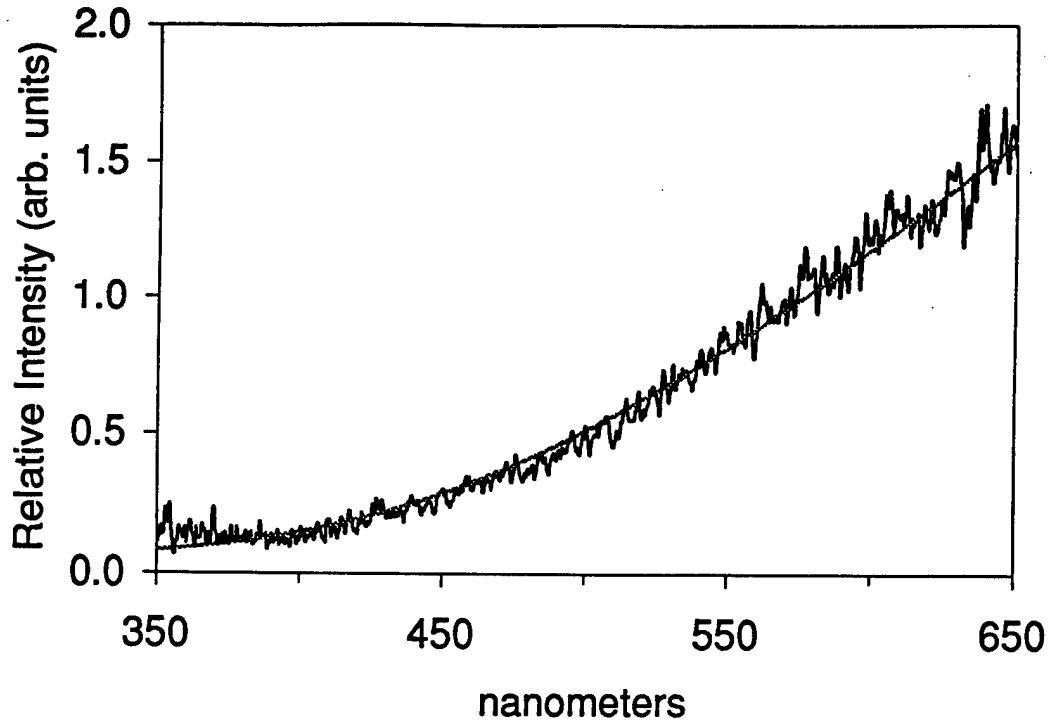


Figure 4. Emission Spectrum Associated With Bubble Collapse and Comparison to a Black-Body Emitter at 2,800 K.

did not attempt to determine absolute irradiance values.) Employing a nonlinear least-squares-fitting routine, the temperature yielding the best fit to the distribution was determined to be 2,800 K. We note that the response function of the fiber-optic-OMA combination, needed to obtain the actual relative intensities from the raw spectral data, was established using a length of fiber that was shorter than that used in the experiment. Because the relative attenuation per length of fiber increases as the wavelength decreases below 500 nm, the temperature derived from the fit is presumably a lower limit. However, correcting this flaw in the data reduction is not expected to significantly change the observation that bubble collapse produces black-body-like emission. We note that this type of intensity distribution is also observed in sonoluminescence (light produced in aqueous solutions by applying acoustic energy to form and collapse cavitation bubbles) [11].

Figure 5 shows the (properly) corrected spectrum for light associated with the luminous wave propagating from the initiation sight. The spectrum is essentially a continuum with a short wavelength onset near 400 nm. However, in this case, synthetic spectra generated by the black-body-based model can not reasonably reproduce this spectrum, with the slope change in the spectral distribution at about 425 nm being inconsistent with the black-body radiation law function. The wavelength onset and range of emission suggest that the spectrum is associated with emission from electronically excited NO_2 [12]. This inference is further supported by the observation of reddish-brown gas (another signature of NO_2) immediately following the passage of the white light.

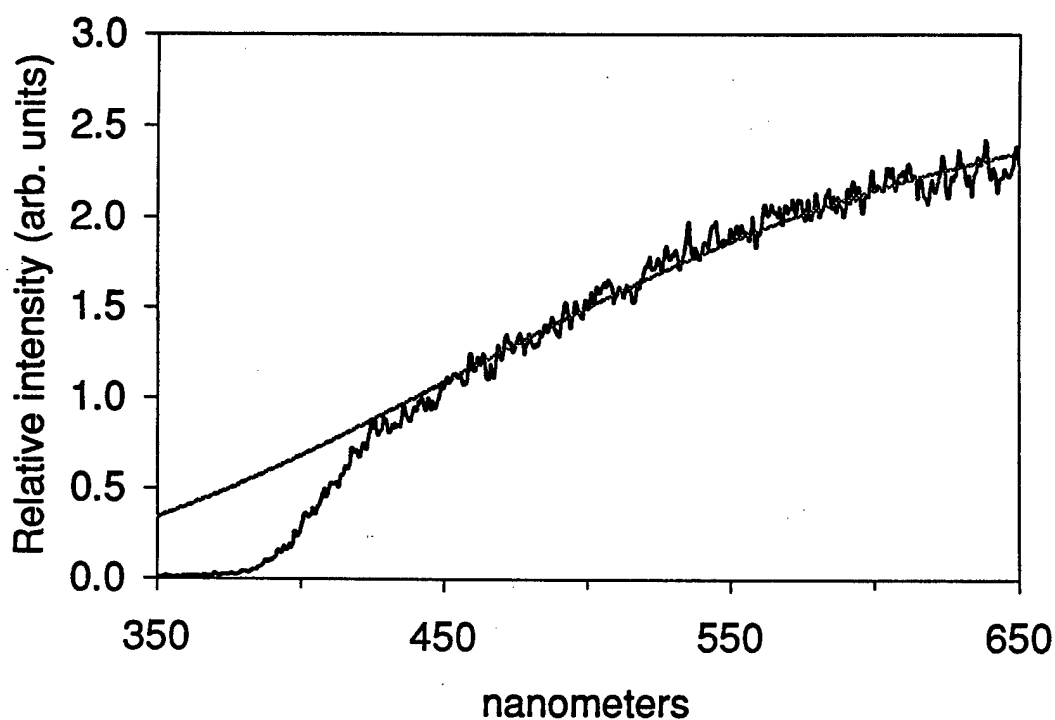


Figure 5. Emission Spectrum Associated With the Luminous Wave and Comparison to a Black-Body Emitter at 3,800 K.

The synthetic spectrum shown for comparison in Figure 5 was generated by fitting the black-body-based model to the $\lambda > 425$ -nm portion of the experimentally obtained spectrum. It is the distribution that would be produced by a black body at 3,800 K. We consider it possible that the good agreement between the model and the spectrum is a result of the medium being “optically

thick" in this wavelength regime. If so, the fit is not a meaningless comparison, as is the case if the medium is not in this limit; rather, it would correspond to the color temperature of the wave. To explore this possibility, a model based on the radiative transfer equation would need to be employed. Unfortunately, a database for the NO₂ rovibronic transitions (line positions, line strengths, and collisional broadening parameters) required for input into the equation has not been established, and, given the complexity of NO₂'s energy level structure, unlikely to be so in the near future.

The attribution to NO₂ would be consistent with expectations based on thermal decomposition studies of XM46 and its components. NO₂ was observed as an early decomposition product in the slow thermal decomposition of HAN in a high-pressure diamond anvil cell [13] and in the rapid thermolysis of HAN in argon atmospheres to 7 MPa [14]. Moreover, such studies suggest a simple pathway to explain the formation of NO₂. It has been proposed that the first step in the decomposition of HAN involves proton transfer from NH₂OH⁺ to NO₃⁻ to produce HNO₃ (nitric acid) and either ammonia oxide or hydroxylamine [15], and nitric acid vapor decomposes via the reaction,



It was considered that the observation of OH, which has a strong (A-X) transition at 308 nm, would provide corroborative, though not conclusive, evidence for this reaction step, but it was not observed.

The production of nitric acid would increase the sensitivity of the propellant, consistent with the increased sensitivity observed in shock-loaded propellant. We also note that nitric acid could be formed without being detected in previous studies. Being colorless, its would be transparent to high-speed photography, and, given that the proton transfer reaction is only slightly endothermic, the reaction could presumably be significantly driven without being detected via shock velocity measurements. Similarly, the lack of evidence for OH in the emission spectrum can be rationalized; (e.g., the process by which nitric acid decomposes may not be energetic enough to populate the OH A state, or the radical may react as soon as it is formed). Unfortunately, nitric acid in solution with HAN, TEAN, and water is not amenable detection via optical spectroscopy, and its formation

(onset) and the extent to which its production is irreversible will be difficult to establish. As an alternative to probing for nitric acid directly, experiments employing diagnostics designed to detect ammonia oxide or hydroxylamine might be instructive.

Beyond being (perhaps) the signature of a reaction product, we consider that the spectra offer some insight into the mechanism driving the induction phase. As noted in previous studies [7], the wave propagates at very high velocity in Figure 2, traveling from the initiation site to the fiber optics, a distance of 20 mm, in approximately 4 μ s. The velocity (5 mm/ μ s) is much faster than the sonic velocity (2 mm/ μ s) of XM46 [16], yet below the Chapman-Jouguet detonation velocity for the propellant. This suggests that the process can be classified as a low-velocity detonation (LVD) [17]. Cavitation is clearly linked with LVD, but the mechanism by which it enables LVD is system specific. In the present case, the extent to which cavitation bubbles form and collapse prior to the arrival of the wave is unknown. Lacking this information, we consider two limits: (1) most of the bubbles formed collapse prior to the arrival of the wave, and (2) the bubbles collapse only upon arrival of the wave. The presumption in the first scenario would be that bubble collapse produces dispersed hot spots that initiate partial propellant decomposition, and that LVD is supported by the chemical state of the mixture. If so, the light emitted by the wave would be expected to be a result of chemiluminescence (the emission from exothermic reactions that produce products in electronically excited states) of which a flame is an example. The presumption in the second scenario would be that the propagation of the wave would depend on the physical state of the liquid. In this case, emission from the wave could have the characteristics of sonoluminescence.

From a thermodynamics standpoint, either the exothermicity of a chemical reaction or the energy concentration produced by bubble collapse could conceivably populate the molecular (or atomic) energy levels needed to produce observable emission at near-UV wavelengths. (Emission at 400 nm requires a process that can partition at least 71 kcal/mol to products.) What is interesting, though, is that neither the sodium D-line transitions at 589 nm nor the OH A-X transitions at 308 nm are observed. These transitions were the dominant features in emission from combusting XM46 sprays at 33 MPa [18]. The lack of signatures attributable to sodium and OH, coupled with the lack of observable gas production or energy release, suggests that the emission from the wave is associated

with sonoluminescence and (perhaps) a decomposition mechanism such as reaction (1) and not chemiluminescence associated with combustion reactions.

However, even if this interpretation is correct, issues remain. For example, the qualitative difference between the spectrum associated with the collapse of an air bubble (Figure 4) and the spectrum associated with the wave could be taken to suggest that decomposition occurs before the wave arrives, but we can not rule out the possibility that the spectral character is associated with a temperature vs. optical density effect. (That is, for a given transition and its carrier density, a wavelength whose intensity is at the optically thick limit for a low temperature could be below this limit at a higher temperature.) Thus, it is still not known whether a chemical change, induced directly by the initial passage of the shock wave, is an important precursor to the shock-induced initiation process. We hope, at some point, to be able to further investigate this question.

4. Summary

The luminous (white) wave observed immediately prior to rapid acceleration of material in flyer plate impact experiments with XM46 was spectrally resolved, and it is considered that the spectrum is attributable to emission from electronically excited NO_2 . For wavelengths greater than 425 nm, the spectrum is well fit as 3,800 K black-body emission, but the validity of this interpretation is uncertain. We suggest that the emission is sonoluminescent rather than chemiluminescent in origin, but the coupling between physical and chemical mechanisms in the shock-induced initiation process remains unresolved.

5. References

1. Lyman, O. R., and J. T. McLaughlin. "Liquid Propellant XM46 Response to Four Different Shaped Charge Jet Attacks." ARL-MR-185, U.S. Army Research Laboratory, Aberdeen Proving Ground, MD, 1994.
2. Lyman, O. R., and O. H. Blake. "Liquid Propellant/Jet Interactions: Container Wall Effects." ARL-TR-670, U.S. Army Research Laboratory, Aberdeen Proving Ground, MD, 1995.
3. Gibbons, G., J. L. Watson, and T. C. Adkins. "Response of Liquid Gun Propellant to Shaped Charge Jet Impact." ARL-TR-1311, U.S. Army Research Laboratory, Aberdeen Proving Ground, MD, 1997.
4. Frey, R., J. Watson, G. Gibbons, V. Boyle, A. Finnerty, W. Lawrence, C. Leveritt, P. Peregino, D. Pilarski, O. Blake, A. Bines, and A. Canami. "Compartmentation Technology for Liquid Propellant (XM46)." ARL-TR-956, U.S. Army Research Laboratory, Aberdeen Proving Ground, MD, 1996.
5. Trott, B. D., H. N. Ebersole, and G. Fenton. "Hugoniot Equation of State and Direct Shock Response of Liquid Propellant XM46." *1994 JANNAF Propulsion Systems Hazards Subcommittee Meeting*, CPIA Publication, 1994.
6. Watson, J., and D. Pilarski. "The Response of Liquid Propellant to Shaped-Charge Jet Impacts- III." *1994 JANNAF Propulsion Systems Hazards Subcommittee Meeting*, JHU/CPIA Publication, 1994.
7. Fishburn, B., and P. Lu. "Safety Hazard and Vulnerability Assessment of XM46 Liquid Propellant." In press at U.S. Army Armament Research, Development, and Engineering Center (ARDEC), Picatinny Arsenal, NJ.
8. Baker, P., A. Canami, and R. Pesce-Rodriguez. "Recovery of Shock-Loaded XM46 Liquid Propellant." ARL-TR-1235, U.S. Army Research Laboratory, Aberdeen Proving Ground, MD, 1996.
9. McQuaid, M. J., H. Burden, and W. Lawrence. "Detection of Chemical Intermediate Formation in XM46 Shock-Loaded via an Electric Gun." ARL-TR, U.S. Army Research Laboratory, Aberdeen Proving Ground, MD, in press.
10. Idar, D., and H. Pederson. Presented at a PM-Crusader survivability workpackage interim progress review, U.S. Army Armament Research, Development, and Engineering Center, Picatinny Arsenal, NJ, 1995.
11. Crum, L. "Sonoluminescence." *Physics Today*, vol. 9, p. 22, 1994.

12. Herzberg, G. "Molecular Spectra and Molecular Structure III. Electronic Spectra and Electronic Structure of Polyatomic Molecules." Van Nostrand, NY, 1966.
13. Van Dijk, C. A., and R. G. Priest. "Thermal Decomposition of HAN at Kilobar Pressures." *Combustion and Flame*, vol. 57, p. 15, 1984.
14. Cronin, J. T., and T. B. Brill. "Thermal Decomposition of Energetic Materials. 8. Evidence of an Oscillating Process during the High Rate Thermolysis of Hydroxylammonium Nitrate, and Comments on the Interionic Interactions." *Journal of Physical Chemistry*, vol. 90, p. 178, 1986.
15. Klein, N. "A Model for the Reactions of the HAN-Based Liquid Propellants." ARL-TR-405, U.S. Army Research Laboratory, Aberdeen Proving Ground, MD, 1994.
16. Constantino, M. "The High Pressure Equation of State of LGP 1845 And LGP 1846." 1986 *JANNAF Propulsion Meeting*, CPIA Publication 455, 1986.
17. *Engineering Design Handbook: Principles of Explosive Behavior*. AMCP-706-180, April 1972.
18. Birk, A., M. McQuaid, and G. Bliesener. "Reacting Liquid Monopropellant Sprays—Experiments With High-Velocity, Full-Cone Sprays in 33 MPa, 500 C Nitrogen." ARL-TR-17, U.S. Army Research Laboratory, Aberdeen Proving Ground, MD, 1992.

NO. OF
COPIES ORGANIZATION

2 DEFENSE TECHNICAL
INFORMATION CENTER
DTIC DDA
8725 JOHN J KINGMAN RD
STE 0944
FT BELVOIR VA 22060-6218

1 HQDA
DAMO FDQ
DENNIS SCHMIDT
400 ARMY PENTAGON
WASHINGTON DC 20310-0460

1 DPTY ASSIST SCY FOR R&T
SARD TT F MILTON
RM 3EA79 THE PENTAGON
WASHINGTON DC 20310-0103

1 OSD
OUSD(A&T)/ODDDR&E(R)
J LUPO
THE PENTAGON
WASHINGTON DC 20301-7100

1 CECOM
SP & TRRSTRL COMMCTN DIV
AMSEL RD ST MC M
H SOICHER
FT MONMOUTH NJ 07703-5203

1 PRIN DPTY FOR TCHNLGY HQ
US ARMY MATCOM
AMCDG T
M FIFETTE
5001 EISENHOWER AVE
ALEXANDRIA VA 22333-0001

1 DPTY CG FOR RDE HQ
US ARMY MATCOM
AMCRD
BG BEAUCHAMP
5001 EISENHOWER AVE
ALEXANDRIA VA 22333-0001

1 INST FOR ADVNCD TCHNLGY
THE UNIV OF TEXAS AT AUSTIN
PO BOX 202797
AUSTIN TX 78720-2797

NO. OF
COPIES ORGANIZATION

1 GPS JOINT PROG OFC DIR
COL J CLAY
2435 VELA WAY STE 1613
LOS ANGELES AFB CA 90245-5500

1 ELECTRONIC SYS DIV DIR
CECOM RDEC
J NIEMELA
FT MONMOUTH NJ 07703

3 DARPA
L STOTTS
J PENNELLA
B KASPAR
3701 N FAIRFAX DR
ARLINGTON VA 22203-1714

1 US MILITARY ACADEMY
MATH SCI CTR OF EXCELLENCE
DEPT OF MATHEMATICAL SCI
MDN A MAJ DON ENGEN
THAYER HALL
WEST POINT NY 10996-1786

1 DIRECTOR
US ARMY RESEARCH LAB
AMSRL CS AL TP
2800 POWDER MILL RD
ADELPHI MD 20783-1145

1 DIRECTOR
US ARMY RESEARCH LAB
AMSRL CS AL TA
2800 POWDER MILL RD
ADELPHI MD 20783-1145

3 DIRECTOR
US ARMY RESEARCH LAB
AMSRL CI LL
2800 POWDER MILL RD
ADELPHI MD 20783-1145

ABERDEEN PROVING GROUND

4 DIR USARL
AMSRL CI LP (305)

NO. OF
COPIES ORGANIZATION

1 PM SRVBLTY SYSTM
SFAE ASM SS M M RYZYI
WARREN MI 48397-5000

1 CDR USA ARDEC
AMSTA AR AEE B D DOWNS
PICATINNY ARSENAL NJ
07806-5000

2 CDR USA ARDEC
AMSTA AR AEE WW P LU
B FISHBURN
PICATINNY ARSENAL NJ
07806-5000

1 CDR USA ARDEC
AMSTA AR EE WW J LANNON
PICATINNY ARSENAL NJ
07806-5000

1 BATTELLE
D TROTT
505 KING AVE
COLUMBUS OH 43201

1 DIR LANL
D IDAR
PO BOX 1633
LOS ALAMOS NM 87545

ABERDEEN PROVING GROUND

30 DIR ARL
AMSRL WM B,
W CIEPICLA
A HORST
M SMITH
AMSRL WM BE,
A BIRK
T COFFEE
J COLBURN
J DESPIRITO
C LEVERITT
T MINOR
S RAY
G WREN
AMSRL WM BC, P PLOSTINS

NO. OF
COPIES ORGANIZATION

AMSRL WM BD,
R BEYER
S BUNTE
B FORCH
K MCNESBY
M J MCQUAID (5 CP)
R PESCE-RODRIGUEZ
AMSRL WM T, W MORRISON
AMSRL WM TC,
P BAKER
R FREY
G GIBBONS
W LAWRENCE
D PILARSKI
J STARKENBERG
J WATSON

REPORT DOCUMENTATION PAGE

Form Approved
OMB No. 0704-0188

Public reporting burden for this collection of information is estimated to average 1 hour per response, including the time for reviewing instructions, searching existing data sources, gathering and maintaining the data needed, and completing and reviewing the collection of information. Send comments regarding this burden estimate or any other aspect of this collection of information, including suggestions for reducing this burden, to Washington Headquarters Services, Directorate for Information Operations and Reports, 1215 Jefferson Davis Highway, Suite 1204, Arlington, VA 22202-4302, and to the Office of Management and Budget, Paperwork Reduction Project (0704-0188), Washington, DC 20503.

1. AGENCY USE ONLY (Leave blank)		2. REPORT DATE May 1998	3. REPORT TYPE AND DATES COVERED Final, July 1995 - January 1996	
4. TITLE AND SUBTITLE UV/Vis Emission From Shock-Loaded Liquid Propellant XM46			5. FUNDING NUMBERS 1L161102AH43	
6. AUTHOR(S) M. J. McQuaid, J. L. Watson, and D. L. Pilarski			8. PERFORMING ORGANIZATION REPORT NUMBER ARL-TR-1672	
7. PERFORMING ORGANIZATION NAME(S) AND ADDRESS(ES) U.S. Army Research Laboratory ATTN: AMSRL-WM-BD Aberdeen Proving Ground, MD 21005-5066			10. SPONSORING/MONITORING AGENCY REPORT NUMBER	
9. SPONSORING/MONITORING AGENCY NAMES(S) AND ADDRESS(ES)			11. SUPPLEMENTARY NOTES	
12a. DISTRIBUTION/AVAILABILITY STATEMENT Approved for public release; distribution is unlimited.			12b. DISTRIBUTION CODE	
13. ABSTRACT (Maximum 200 words) In flyer plate impact experiments conducted to study the response of the liquid propellant XM46 to shock loading, it had been observed that, in cases where the sample reacted violently, a luminous wave would travel at high velocity across a free-surface or container boundary prior to significant acceleration of materiel. This report presents the results of experiments in which the ultraviolet (UV) and visible (Vis) radiation from this wave were spectrally resolved. The emission spectrum was found to be a broad, nearly structureless continuum that extends from a short wavelength onset near 400 nm to the long wavelength limit of the detection system at approximately 800 nm. It is considered that this signature is attributable to emission from electronically excited NO ₂ . Mechanisms that might explain the experimental observations are discussed.				
14. SUBJECT TERMS liquid propellant, shock sensitivity, UV-visible emission spectroscopy, XM46			15. NUMBER OF PAGES 22	
17. SECURITY CLASSIFICATION OF REPORT UNCLASSIFIED			16. PRICE CODE	
18. SECURITY CLASSIFICATION OF THIS PAGE UNCLASSIFIED		19. SECURITY CLASSIFICATION OF ABSTRACT UNCLASSIFIED		20. LIMITATION OF ABSTRACT UL

INTENTIONALLY LEFT BLANK

USER EVALUATION SHEET/CHANGE OF ADDRESS

This Laboratory undertakes a continuing effort to improve the quality of the reports it publishes. Your comments/answers to the items/questions below will aid us in our efforts.

1. ARL Report Number/Author ARL-TR-1672 (McQuaid) Date of Report May 1998

2. Date Report Received _____

3. Does this report satisfy a need? (Comment on purpose, related project, or other area of interest for which the report will be used.) _____

4. Specifically, how is the report being used? (Information source, design data, procedure, source of ideas, etc.) _____

5. Has the information in this report led to any quantitative savings as far as man-hours or dollars saved, operating costs avoided, or efficiencies achieved, etc? If so, please elaborate. _____

6. General Comments. What do you think should be changed to improve future reports? (Indicate changes to organization, technical content, format, etc.) _____

CURRENT
ADDRESS

Organization

Name E-mail Name

Street or P.O. Box No.

City, State, Zip Code

7. If indicating a Change of Address or Address Correction, please provide the Current or Correct address above and the Old or Incorrect address below.

OLD
ADDRESS

Organization

Name

Street or P.O. Box No.

City, State, Zip Code

(Remove this sheet, fold as indicated, tape closed, and mail.)
(DO NOT STAPLE)

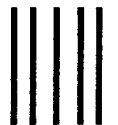
DEPARTMENT OF THE ARMY

OFFICIAL BUSINESS

BUSINESS REPLY MAIL
FIRST CLASS PERMIT NO 0001,APG,MD

POSTAGE WILL BE PAID BY ADDRESSEE

**DIRECTOR
US ARMY RESEARCH LABORATORY
ATTN AMSRL WM BD
ABERDEEN PROVING GROUND MD 21005-5066**



**NO POSTAGE
NECESSARY
IF MAILED
IN THE
UNITED STATES**

